

SIMULATIONS OF CORAL GRAVEL ACCUMULATION IN THE OPEN-CUT CAUSEWAY IN FONGAFALE ISLET OF FUNAFUTI ATOLL, TUVALU

Daisaku Sato¹ and Hiromune Yokoki²

Numerical simulations of coral gravel transportation were conducted to estimate the accumulation possibility in the gap which is formed by the open-cutting of the causeway in Fongafale Islet of Funafuti Atoll. In the numerical simulation of wave field, the high wave conditions were considered in the boundary condition. Calculated morphological change in the gap showed that the extremely large accumulation of coral gravels was not estimated. However the southern edge of the gap had large accumulation locally. In the middle and northern part of the gap accumulated gravel formed thin layer. Because the calculated morphological change of lower wave condition showed large accumulation as well as the results of higher wave condition, it is estimated that the direction of incident wave is important factor of the accumulation. The simulated result indicated that the rapid blockade of the gap would not be caused by accumulation of coral gravels. However, the periodic maintenance of the gap is required for keeping the function of the gap continuously.

Keywords: coral gravel transportation; numerical simulation; Funafuti atoll

INTRODUCTION

Funafuti Atoll, Tuvalu has the low-lying islands constructed by foraminifers, coral sands and gravels (Yamano et al., 2005; Yokoki et al., 2005). The islands form on the ring-shaped shallow reef. Atoll islands have a calm lagoon that is enclosed by a circular shallow reef. The water depth of lagoon is tens of meters and it is quite shallow compared with the ocean. Fongafale Islet on the eastern side of the atoll has a problem of coastal erosion on the lagoonal sandy beach, which is caused by poor sediment supplies from ocean-side reef-flat. Coastal erosion is a big problem in other atoll islands such as Majuro Atoll, Marshall Islands (Sato and Yokoki, 2010). In order to countermeasure the beach erosion, hard structures such as groins, vertical walls and dikes are constructed in the coast generally. However the natural island maintenance system that is consisted by sediment production by reef-living organisms, sediment transportation and sediment accumulation would be collapsed by constructions. In the view of sustainable conservation of the island coast the system should be maintained. Understanding of natural processes of the sediment transport is the fundamental information for controlling the coastal erosion. However, the interaction between morphological changes of the islands and the driving forces such as waves is not considered enough (Yokoki et al., 2005; Kench and Brander, 2006).

On the other hand, it is indicated that atoll islands have high vulnerability to environmental changes such as sea-level rise (Leatherman, 1997; Yamano et al., 2005). Acceleration of the coastal erosion caused by the future sea-level rise in Majuro Atoll, Marshall Islands is estimated by Sato and Yokoki, 2010. In the Funafuti Atoll, the increase of nearshore wave height due to the sea-level rise is indicated by the results of the numerical simulation. Thus the future nearshore environment of the atoll island would change large. Hard constructions are not desirable in the atoll islands because the maintenance of its functions against the sea-level rise is not easy in economical and technical factors. In a long-range point of view, the natural process of the island formation should be maintained and enhanced for sustainable conservation of the island.

Sato et al.(2012) focused on the possibility of increasing the lagoonal sediment transport due to excavating the causeway which connects Fongafale to a northern island. Active production of sand by foraminifers is observed in the ocean-side reef-flat of the causeway. Numerical simulation of sediment transport conducted by Sato et al.(2012) indicated that the excavation of the causeway is a good measure to increase the lagoonal longshore sediment transport supplied in the ocean-side active sediment production zone. On the other hand, coral gravels are also major sediment which is produced on the ocean-side reef-flat and their movements are quite important for the maintenance and the sediment transport process through the gap (the open-cut causeway). In this study, numerical simulation was conducted to understand movement of coral gravels through the gap.

¹ Department of Civil and Environmental Engineering, Tokyo Denki University, Ishizaka Hatoyama, Hiki-gun, Saitama, 350-0394, Japan

² Department of Urban and Civil Engineering, Ibaraki University, 4-12-1 Nakanarusawa, Hitachi, Ibaraki, 316-8511, Japan

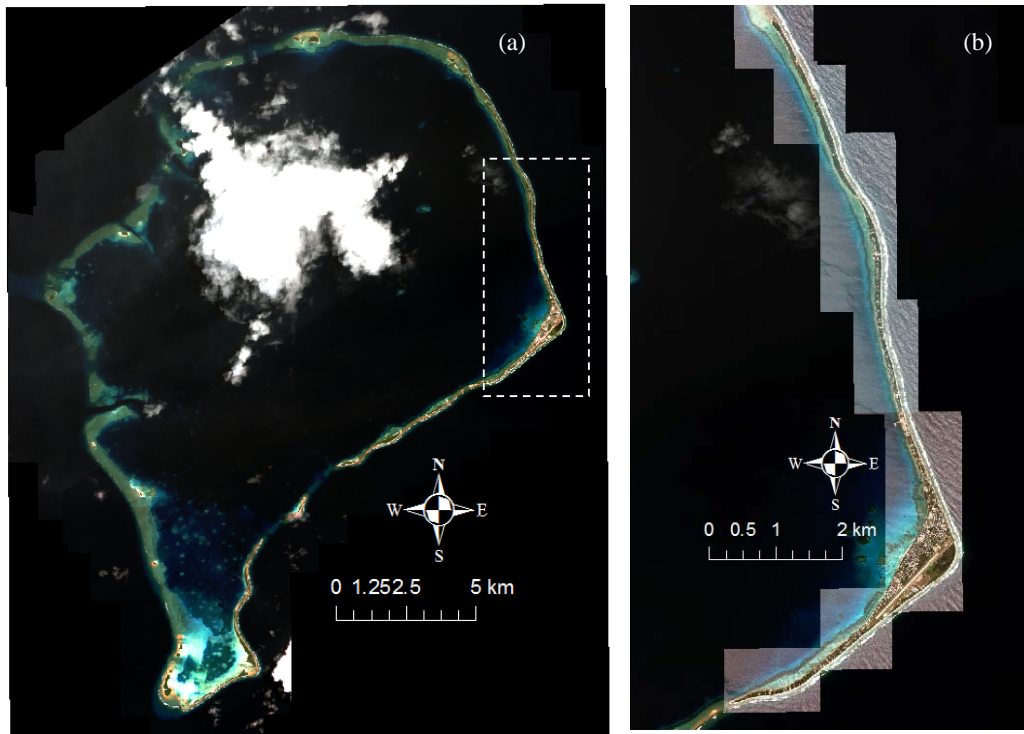


Figure 1. (a) Satellite image of Funafuti atoll. Dotted area shows Fongafale islet. (b) Expanded image of Fongafale islet.

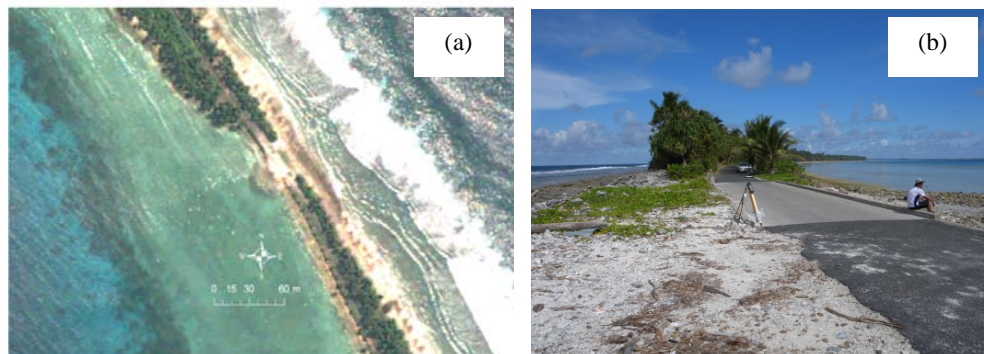


Figure 2. (a) Expanded image of the causeway (b) Causeway pictured from north

FONGAFALE ISLET, FUNAFUTI ATOLL

Tuvalu is located in South Pacific ($5^{\circ}40' \sim 10^{\circ}47'S$, $176^{\circ}06' \sim 179^{\circ}50' E$) and has nine atolls. Funafuti atoll, which is the capital of Tuvalu, is almost 20km width from north to south and east to west (Fig. 1(a)). Fongafale islet located in the eastern part of the atoll is the central part for residence and governmental offices (Fig. 1(b)). Funafuti atoll has two passages in the east and west reefs, and they enable the oceanic waves to pass into the lagoon with less dispersion. The causeway is the narrow artificial construction locates in the northern part of Fongafale Islet (Fig. 2(a), (b)).

Figure 3 shows the profiles of causeway that measured by our project in Mar. 2009 and Apr. 2010 respectively. The profiles indicated the topography of the causeway that is about 20m width and 2m high from M.S.L. There is a difference in level by 20cm between lagoon-side and ocean-side. The reef-flat of ocean-side is a little higher than that of lagoon-side. Two profiles showed that the reef-flat in the both side of causeway had small morphological change between 2009 and 2010.

Dominant material around the ocean-side beach of causeway is coral gravel. The lagoon-side coast has a lot of large coral gravel. In addition, a little accumulation of sand is recognized from the picture.

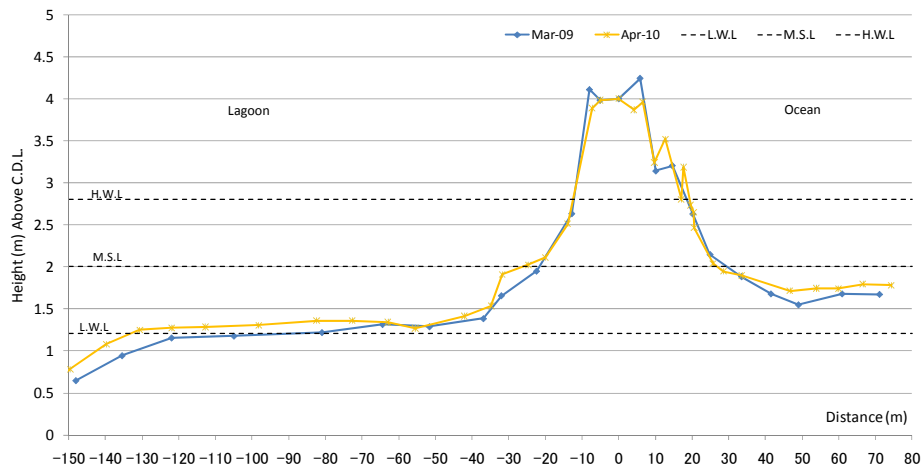


Figure 3. Measured profiles of the causeway (March-2009 and April-2010)

These gravels would have been transported from ocean-side to lagoon-side when waves and tide were extremely high condition. Then, the lagoon-side of the causeway has a rapid slope from road to reef-flat. On the other hand, the ocean-side of the causeway has a lot of coral gravel, and distinctive topography such as step continues by almost 5m from road. This distinctive shape of topography can be recognized from distribution of vegetation indicated in Fig 2. The not flat line of the ocean-side slope in Fig 3 indicates accumulation of the huge rock of coral. The high-density habitat of foraminifers is located in the offshore reef-flat that is more far from the ocean-side edge of the profiles of Fig 3. Sand with firm spine accumulated a little near the ocean-side shoreline. Thus, the dominant sediments around the causeway are coral gravel, and the ocean-side has a lot of gravel.

CALCULATION METHOD

Calculation Method of Wave Field

SWAN(Simulating WAVes Nearshore), which was constructed by Delft University, Netherlands, is the numerical model simulating the nearshore wave transformation such as wave refraction, wave diffraction and wave breaking and it was applied to calculate the wave field in Funafuti atoll. SWAN is based on the spectral action balance equation. In the model, waves are described as the two dimensional wave variance spectral densities. The basic equation of SWAN that is described in Booij et al (1999) is:

$$\frac{\partial}{\partial t} N + \frac{\partial}{\partial x} c_x N + \frac{\partial}{\partial y} c_y N + \frac{\partial}{\partial \sigma} c_\sigma N + \frac{\partial}{\partial \theta} c_\theta N = \frac{W}{\sigma} \quad (1)$$

Where $N (=S/\sigma)$: the action density, c_x, c_y : the propagation velocity in horizontal space, c_σ, c_θ : the propagation velocity in spectral space. The propagation velocities are same those of the energy balance equation. The first term of Eq. 1 indicates the time-depending change of the action density. The second and third terms indicate energy propagation in horizontal space. The fourth and fifth terms indicate energy propagation in spectral space. The right-hand side of Eq. 1 contains the source/sink term that represents all physical processes, which generate, dissipate, or redistribute wave energy. Eq. 1 is based on the energy balance equation (e.g., Hasselmann et al, 1973).

Calculation Domain

This simulation focused on the transportation of widely distributed sand on the reef-flat. Although there are many equations for evaluating the volume of sediment transportation, the calculation model of local sediment transport rate was adopted in this study because the model can treat a planar distribution of sediment transportation. Sato and Kabiling (1994) proposed the calculation method of net volume of sediment transport which is constructed by the calculation of local sediment transport rate from bottom velocity at each moment, and the round period integration of the calculated rate. In the proposed method, the sediment transport rate divided to the suspended load and the bed load, and the sediment transport is generated when Shields number is over the critical Shields number. Equations of each sediment transport are described as:

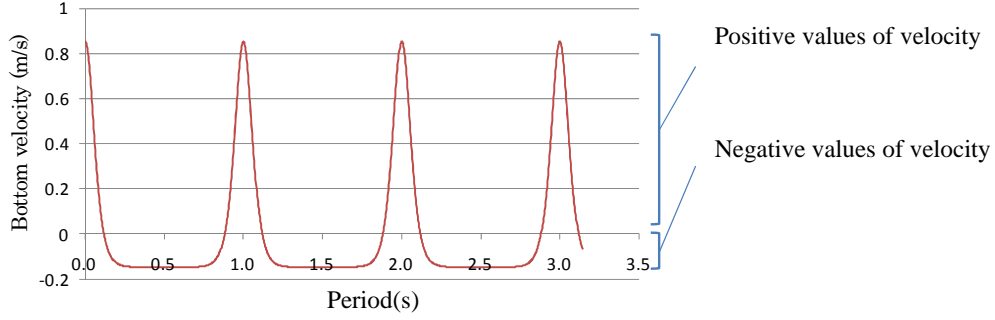


Figure 4. Example of the bottom velocity of Cnoidal wave

$$\frac{\bar{q}_B(t)}{\sqrt{(\rho_s / \rho - 1)gD_s^3}} = \alpha_B |\Psi(t)|^{0.5} \max(\Psi(t) - \Psi_c, 0) \cdot \frac{\bar{u}_b(t)}{|\bar{u}_b(t)|} \quad (2)$$

$$\frac{\bar{q}_S(t)}{\omega_S D_S} = \alpha_S \max(\Psi(t) - \Psi_c, 0) \cdot \frac{\bar{u}_b(t)}{|\bar{u}_b(t)|} \quad (3)$$

Where, D_s : sediment diameter, ρ_s, ρ : density of sediment and water (=2.56, 1.03), $\Psi(t)$: Shields number, $\Psi_c(t)$: critical Shields number, α_B, α_S : coefficient(=1.0, 3.5), ω_S : settling velocity of sediment (calculated by Sawaragi and Deguchi (1996)), u_b : bottom velocity at a moment. Shields number was calculated the equation:

$$\Psi(t) = \frac{f_w}{2} \frac{\bar{u}_b(t)^2}{(\rho_s / \rho - 1)gD_s} \quad (4)$$

Here, f_w is share velocity calculated by the equation as:

$$f_w = \exp(-7.53 + 8.07 \frac{|\bar{u}_b(t)|}{\sigma \cdot z_0})^{-0.1} \quad (5)$$

Where, σ : angular frequency ($\sigma=2\pi/L$), z_0 : roughness length (=sediment diameter), critical Shields number $\Psi_c(t)$ was calculated using the momentary bottom velocity and the critical share velocity by Eq. 6 using d (the diameter of sediment).

$$\begin{aligned} d \geq 0.303\text{cm} & : u_{*c}^2 = 80.9d \\ 0.118 \leq d \leq 0.303\text{cm} & : u_{*c}^2 = 134.6d^{\frac{31}{22}} \\ 0.0565 \leq d \leq 0.118\text{cm} & : u_{*c}^2 = 55.0d \\ 0.0065 \leq d \leq 0.0565\text{cm} & : u_{*c}^2 = 8.41d^{\frac{11}{32}} \\ d \leq 0.0065\text{cm} & : u_{*c}^2 = 226.0d \end{aligned} \quad (6)$$

The momentary bottom velocity, which is needed in Eq. 2 and 3, should be assumed from the calculated wave situation such as the significant wave height and the mean wave direction, because the wave model that was used in this study was constructed based on the wave spectrum. Because the assumption of the Small Amplitude Waves theory makes the wave-shape as sine function and it adjusts the net sediment transportation to zero, the cnoidal waves that correspond to quite shallow water waves, was adopted for assuming the wave's shape (Fig. 4).

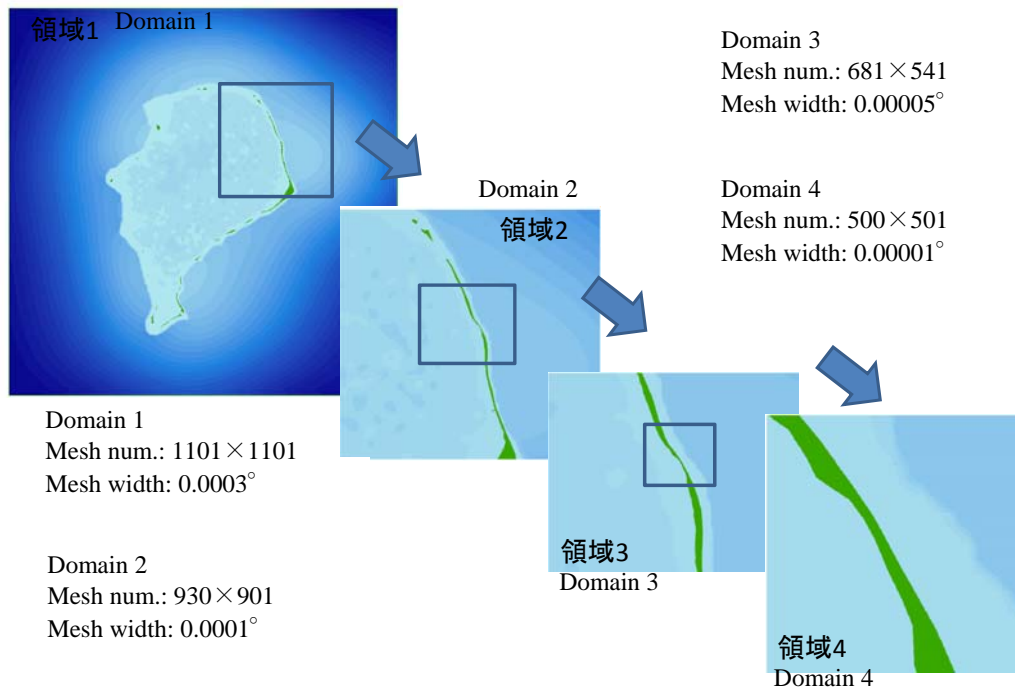


Figure 5. Calculation domain

Calculation Domain

The multi-scale nesting method was adopted as the setting of the calculation domain in order to calculate around the causeway by high resolution. Figure 5 indicated the calculation domain at each nesting scale. There are four scales from domain 1 and domain 4. Domain 1 includes whole of Funafuti atoll and fits to the input outer boundary condition. Mesh size is 0.0003degree, which equal about 30m. Oceanic water depth was constructed by ETOPO2, which was the global bathymetrical and topographical data with two minutes meshes. Lagoonal water depth was digitized from a chart. After these data were overlaid on the GIS system, the combined bathymetric data was interpolated to desirable resolution. In the constructed bathymetric data, the elevation of the islets and the water depth on the reef-flat were set to 2m and 1m uniformly.

Mesh size of domain 2 is 0.0001degree (almost 10m). This domain includes from the north tip of Fongafale islet and middle of Fongafale (southern part of Catalina ramp). Not only the calculation of the wave field but also the calculation of the sediment transport was carried out using this domain.

Domain 3 has 0.00005° (about 5m) of resolution and it provides the boundary condition of wave situation to domain 4. Domain 4, which has 0.00001° (about 1m) of resolution, includes modified topography by open cutting of the causeway. The sediment transportation between Domain 2 and Domain 4 are connected in the calculation.

Boundary Condition

Calculation of the wave field is required the boundary condition of waves and winds situation. Although SWAN needs the significant wave height, the period of significant wave and the mean wave direction, there is no observed wave situation for the boundary condition around Funafuti atoll. In addition, the wave field calculation is required of the values of many spaces and time, therefore the re-analysis data of global wave and wind situation simulated by ECMWF (European Center for Middle-Range Weather Forecasts) was adopted for the boundary conditions. The datasets of ERA-40 and Interim were used for constructing the boundary condition for the wave field calculation. ERA-40 and Interim was calculated based on the observed data by 1.5° grid. Provided datasets include the wave situation every 6 hours. ERA40 and Interim contains the numerical result from January 1, 1957 to August 31, 2002 and from January 1, 1989 to September 31, 2009 respectively (As of December 2010). In this study, the dataset from January 1, 1957 and December 31, 2009 was used for calculating the

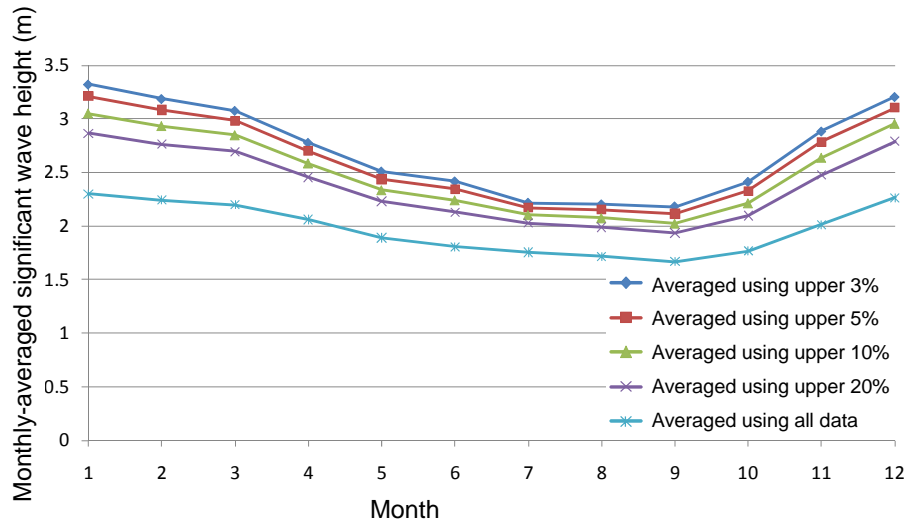


Figure 6. Boundary condition for wave calculation in domain 1

| Month | Upper 3% | Upper 5% | Upper 10% | Upper 20% |
|-------|----------|----------|-----------|-----------|
| Jan | 1 | 1 | 3 | 6 |
| Feb | 1 | 1 | 2 | 5 |
| Mar | 1 | 1 | 3 | 6 |
| Apr | 1 | 1 | 3 | 6 |
| May | 1 | 1 | 3 | 6 |
| Jun | 1 | 1 | 3 | 6 |
| Jul | 1 | 1 | 3 | 6 |
| Aug | 1 | 1 | 3 | 6 |
| Sep | 1 | 1 | 3 | 6 |
| Oct | 1 | 1 | 3 | 6 |
| Nov | 1 | 1 | 3 | 6 |
| Dec | 1 | 1 | 3 | 6 |

monthly-averaged values of the significant wave height, the period of significant wave height and the mean wave direction. In Addition, it is considered that the coral gravel will be transported in the high wave situation. In this study, the monthly-averaged datasets using high rank of data: 0.3, 0.5, 10 and 20% were adapted to the boundary condition of wave field simulation (Fig. 6). This average process enables to contain the high wave influence. Action days of each boundary condition are indicated in Table 1.

The boundary conditions of wind situation were calculated by the observed data in the lagoonal coast of Fongafale islet provided by the SEAFRAME project conducted by Australian government. The acquired data is the observed mean wind speed and mean wind direction every one hour from 0:00 UTC May 1, 1993 to 23:00 UTC December 31, 2008. Monthly-averaged wind speed and wind direction were calculated for the boundary conditions.

The wave field was calculated in all domains of Fig. 5 and the topographic change was calculated in domain4 only. Feedback of topographic change was considered in domain 4. The gravel volume supplied in ocean-side reef-flat was given amount of one twelfth of $0.002\text{m}^3/\text{year}$ as a test case. The calculation was carried out for a year with the condition that the island mesh was set as the unmovable as well. In addition, the calculation was conducted using the normal boundary condition shown in Fig. 6 (as shown in 'Averaged using all data') in order to compare with other results. The calculated topography was discussed by focusing on the profile of the causeway from north to south (Fig. 7).

CALCULATION RESULTS OF GRAVEL TRANSPORTATION

Figure 8 indicates the profiles of calculated topographical change using the normal monthly-averaged boundary condition. The calculated result shows that the active gravel transportation was not caused. Although quite small accumulation was detected in the southern part of the gap, the

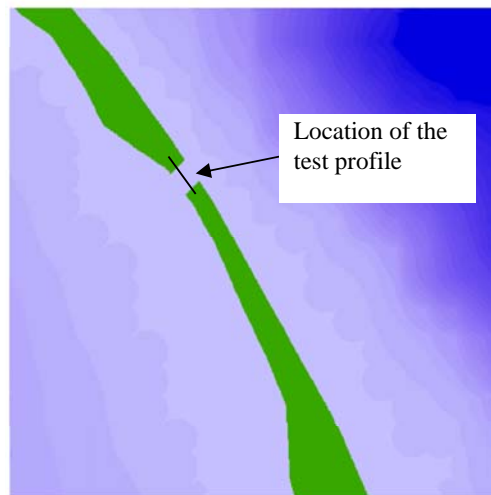


Figure 7. Location of the profile

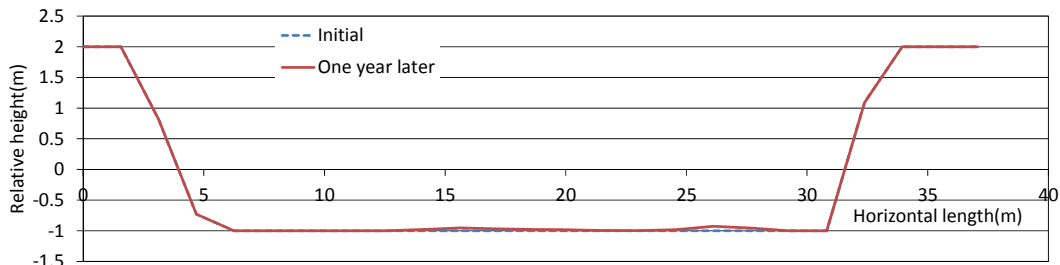


Figure 8. Calculated morphological changes on the gap in normal averaged wave condition.

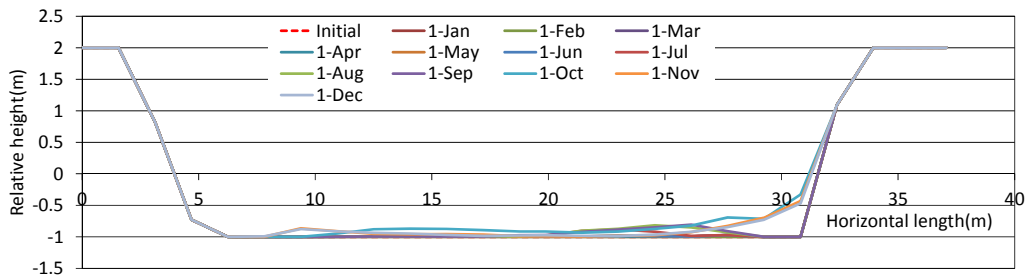


Figure 9. Calculated morphological changes on the gap under the 3% higher waves condition.

topographical change would not be affected to the function of the gap. Thus the function of the gap is maintained in daily calm wave condition.

Calculated topographic profiles calculated using the boundary condition averaged by the high rank of 0.3% is indicated in Fig. 9. The topographic profiles indicate first of each month. Although the boundary condition included the highest range of the re-analyzed waves, the extremely large accretion was not identified from the calculated result. Comparatively many gravel was transported to the open cut area of the causeway in spite of the calculation period that is only a day. The accumulated thickness in the edge of the gap was about 50cm. However, the supplied volume of gravel would be an overabundance condition compared with the realistic value because the sediment supply was adopted every month in the calculation. Thus, this result indicated that the blockade of the open cut causeway would not be caused even if the gravel were supplied every month enough.

Figure 10 shows the topographic profiles which were calculated using the boundary condition averaged by the high rank of 0.5%. A little accretion was identified in the edge of southern part. The middle part of the open cut is similar to the result of the high rank of 0.3%. Although the wave height of boundary condition in the high rank of 0.3% was higher than that of 0.5%, and the calculating

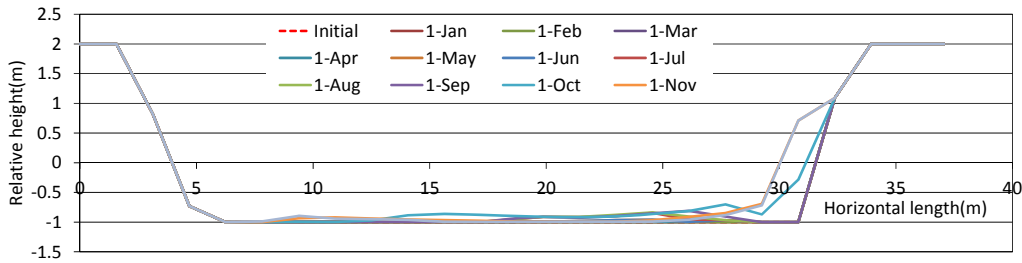


Figure 10. Calculated morphological changes on the gap under the 5% higher waves condition.

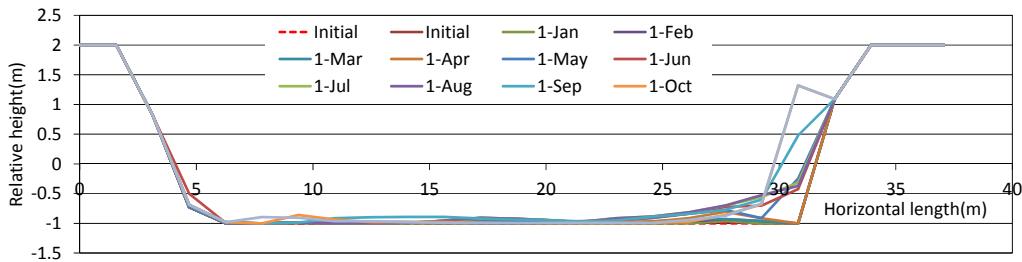


Figure 11. Calculated morphological changes on the gap under the 10% higher waves condition.

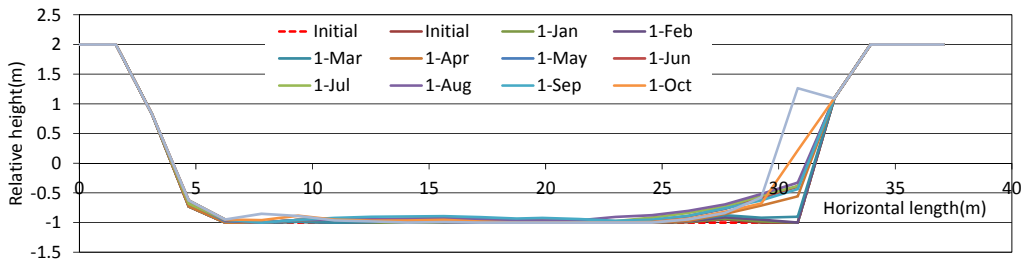


Figure 12. Calculated morphological changes on the gap under the 20% higher waves condition.

period in each condition was same as a day, the morphological change in the rank of 0.5% was larger than that of 0.3%. It was considered that these results were caused by the differences of the incident wave direction. In this case, it seemed that the wave direction changed southern ward because the southern edge of the island has accretion. Although the incident wave height decreased the wave height around the causeway, the wave direction changed the direction of sediment transport and it concentrated the accretion in the southern edge of the island. Although the accretion increased in this boundary condition, it seems that the supplying condition of gravel is overestimated so that the possibility of blockade is extremely low.

In the Fig. 11 the topographic profiles calculated using the boundary condition averaged by the high rank of 10% is showed. The southern tip of the open cut area has accretion same as Fig. 10. In addition, the thin layer of accreted gravel was identified from north to middle in the area. In this case, the calculating period is 3 days, which is three times of the boundary condition of the high rank of 0.3 and 0.5%. Then, the morphological change was caused by the integration of the small accretion. Accreted area is limited in the southern edge of the open cut area so that it is considered that the accretion will not obstruct the sediment transportation.

Figure 12 shows the topographic profiles calculated using the boundary condition averaged by the high rank of 20%. This case has the accreted area in the southern edge of the island as well. However, the accreted layer in north and middle is thin so that the sediment transportation will not be obstructed. Thus, the numerical examination on transportation of coral gravel using four scenarios of boundary condition identified that there is extremely low possibility of both the blockade and the obstruction of sediment transport.

The large accumulation in the edge of the gap was detected in the 0.3% and 0.5% case. Although the wave height of boundary condition in case of 0.3% was higher than that of 0.5%, and the calculating period in these two cases were same, the morphological change in 0.5% was larger than that of 0.3%. It is assumed that the large accretion in the case of 0.5% was caused by the difference of incident wave direction. In the middle of the gap the thin layer of accumulated coral gravels was also formed in this case. The thickness of the thin layer was about 20cm in the both cases. The characteristics of accretion were same with the morphological change in the case of 0.3%. On the other hand, the quite large accumulation was calculated in the lower wave cases shown in Fig. 11 and 12. However, the large accretion was detected in only a part of the gap. These results revealed the rapid blockade of the open-cut causeway would not be caused even in the high wave condition.

CONCLUSION

Numerical simulations of the coral gravels movement on the excavated causeway were conducted to discussing the possibility of blockade of excavated causeway. In the simulation the monthly high wave condition were included in the boundary condition. Conclusions of this study are shows as below.

- In the all of simulation case, coral gravels supplied in the ocean-side reef-flat were transported toward the excavated causeway.
- In the simulation case of higher wave conditions that are 3% and 5%, the accumulated gravel formed thin layer on the gap. In the case of 5% the southern edge of the gap the gravel was accumulated large.
- Simulation result of lower wave condition case shows that the southern edge of the gap had quite large accumulation.
- The thin layer of coral gravels was formed on the middle field of excavated causeway.
- The simulated results showed that the rapid blockade of the open-cut causeway would not be caused by accumulation of gravel. However, periodic removal of coral gravels will be required in order to maintain the function of the gap.

REFERENCES

- Booij, N.R., C. Ris and L.H. Holthuijsen. 1999. A third-generation wave model for coastal regions 1. Model description and validation. *Journal of Geophysical Research*, 104, C4, 7649-7666.
- Hasselmann, K., T.P. Barnett, E. Bouws, H. Carlson, D.E. Cartwright, K. Enke, J.A. Ewing, H. Gienapp, D.E. Hasselmann, P. Kruseman, A. Meerburg, P. Muller, D.J. Olbers, K. Richter, W. Sell and H. Walden. 1973. Measurement of wind-wave growth and swell decay during the Joint North Sea Wave Project(JONSWAP), *Dtsch. Hydrogr. Z. Suppl.*, 12, A8.
- Kench, P.S., and R.W. Brander. 2006. Wave processes on coral reef flats: Implications for reef geomorphology using Australian case studies, *Journal of Coastal Research*, 22, 1, 209–223.
- Leatherman, S.P. 1977. Sea-level rise and small island states: An overview, *Journal of Coastal Research*, Special Issue 24, 1–16.
- Sato, S. and M. B. Kabling. 1994. A Numerical Simulation of Beach Evolution based on a Nonlinear Dispersive Wave-Current Model, *Proc. of the Inter. Conf. on Coastal Eng.*, No 24, 2557-2570.
- Sato, D. and H. Yokoki. 2010. Numerical calculation on shoreline conservation in Majuro Atoll, Marshall Islands, *Proceedings of 32nd International Conference on Coastal Engineering*, pp.1-14.
- Sato, D., H. Yokoki and H. Kayanne. 2012. Improvement of sediment transport by excavation of causeway in Funafuti Atoll, Tuvalu, *Poster presentation of the Inter. Conf. on Coastal Eng. 2012*, Santander.
- Sawaragi, T. and I. Deguchi. 1996. 新編海岸工学, 共立出版株式会社, pp.122. (In Japanese)
- Yamano, H., H. Kayanne, and M. Chikamori. 2005. An Overview of The Nature and Dynamics of Reef Islands, *Global Environmental Research*, 9(1), 9-20.
- Yokoki, H., H. Kayanne, D. Sato, Y. Minami, S. Ando, H. Shimazaki, T. Yamaguchi, M. Chikamori, A. Ishoda, and H. Takagi. 2005. Comparison between Longshore Sediment Transport Due to Waves and Long-term Shoreline Change in Majuro Atoll, Marshall Islands, *Global Environmental Research*, 9(1), 21-26.